Journal of Power Sources 251 (2014) 122–129

Contents lists available at ScienceDirect

Journal of Power Sources

journal homepage: www.elsevier.com/locate/jpowsour

Room temperature cold sprayed TiO_2 scattering layer for high performance and bending resistant plastic-based dye-sensitized solar cells

Xue-Long He [a], Guan-Jun Yang [a,*], Chang-Jiu Li [a,*], Cheng-Xin Li [a], Sheng-Qiang Fan [b]

[a] State Key Laboratory for Mechanical Behavior of Materials, School of Materials Science and Engineering, Xi'an Jiaotong University, Xi'an, Shaanxi 710049, PR China
[b] School of Chemistry & Molecular Biosciences, The University of Queensland, QLD 4072, Australia

HIGHLIGHTS

- Adhesion between scattering layer and NC layer was important for high efficiency.
- NC + RTCS cell showed both higher efficiency and bending resistance than NC + SD cell.
- The effect of scattering layer much depends on TiO_2 NC layer thickness.
- Efficiency of 5.24% was achieved for plastic-based DSC using RTCS scattering layer.

GRAPHICAL ABSTRACT

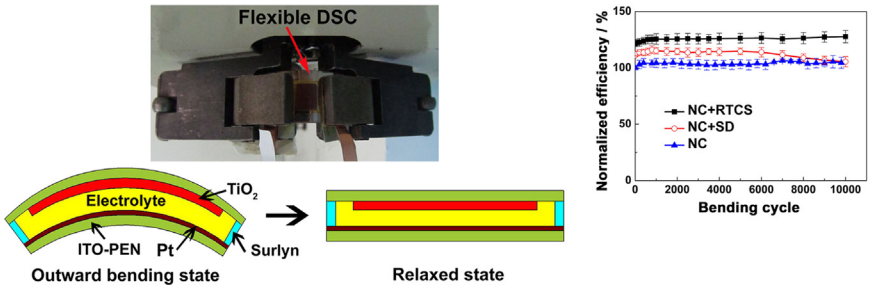

ARTICLE INFO

Article history:
Received 10 July 2013
Received in revised form
12 October 2013
Accepted 3 November 2013
Available online 15 November 2013

Keywords:
Dye-sensitized solar cells
Room temperature cold spray
Scattering layer
Adhesion
Bending resistance

ABSTRACT

High efficiency and flexibility of plastic-based dye-sensitized solar cells (DSCs) are the necessary prerequisites for industrial applications. In this study, light scattering layers are prepared to improve the efficiency and bending resistance of the plastic-based DSCs by both room temperature cold spraying (RTCS) and spray deposition (SD) method. The effect of the adhesion between the TiO_2 scattering layer and TiO_2 nanocrystalline (NC) layer on both the energy conversion efficiency and bending resistance of the plastic-based DSCs are investigated. Results show that both RTCS-TiO_2 and SD-TiO_2 scattering layers yield much higher light-reflecting ability than the TiO_2 NC layer. However, the adhesion between the TiO_2 scattering layer and TiO_2 NC layer for the NC + RTCS cell is higher than the NC + SD cell. The better adhesion results in higher efficiency and better bending resistance for the NC + RTCS cell than the NC + SD cell. In addition, it is found that the increasing ratio of the energy conversion efficiency for the plastic-based DSCs through the introduction of TiO_2 scattering layer decreases significantly with increasing the thickness of TiO_2 NC layer. By using the TiO_2 NC layer with an optimized thickness, a highest efficiency of 5.24% is achieved for the plastic-based DSCs using an RTCS-TiO_2 scattering layer.

1. Introduction

Recently, there is an increasing interest in replacing the rigid glass-based dye-sensitized solar cells (DSCs) by plastic substrates due to light weight, flexibility of shape, suitability for low cost roll-to-roll production [1]. However, the temperature limits of plastic substrates (ca. 150 °C) usually preclude high-temperature process and organic binders usage for the plastic-based DSCs [2]. Compared

* Corresponding authors. Tel.: +86 29 82665299; fax: +86 29 82660970.
E-mail addresses: ygj@mail.xjtu.edu.cn (G.-J. Yang), licj@mail.xjtu.edu.cn (C.-J. Li).

0378-7753/$ – see front matter © 2013 Elsevier B.V. All rights reserved.
http://dx.doi.org/10.1016/j.jpowsour.2013.11.003

with the conventional rigid DSCs, the photo-to-electric energy conversion efficiency of the plastic-based DSCs is relatively low. So far, extensive research has been conducted to improve the photo-to-electric energy conversion efficiency of the plastic-based DSCs [3–9]. A commonly-used way is to add a scattering layer composed of large particles (100–400 nm in diameter) on the TiO_2 nanocrystalline (NC, 10–30 nm in diameter) layer [10,11]. The function of the scattering layer is to scatter the transmitted light back to the TiO_2 NC layer and thereby improve the conversion efficiency of the solar cells. Therefore, to effectively improve the efficiency, the scattering layer should have a high light-reflecting ability. Besides the energy conversion efficiency, the mechanical properties, especially the bending resistance, is also very important for the practical application of plastic-based DSCs [12]. However, to the best of our knowledge, there are few reports concerning the bending performance of the plastic-based DSCs using the photoanode with a scattering layer. To prepare the plastic-based DSCs with high bending resistance, the adhesion between the NC layer and scattering layer should be strong enough to avoid the cracking and spalling off the scattering layer.

Based on our previous results, room temperature cold spraying (RTCS, also called vacuum cold spray) process can be used to prepare well-connected TiO_2 films on plastic substrate [13]. In RTCS method, the dry particles are accelerated to a high velocity in a low-pressure (100–1000 Pa) deposition chamber. During deposition, the impact of high velocity powder particles on the substrate generates a high pressure pulse, resulting in the strong adhesion between the coating and substrate [14]. This feature makes RTCS a promising method to solve the problem of the adhesion between the TiO_2 NC layer and scattering layer.

Another issue for the scattering layer is the increasing ratio of the conversion efficiency of DSCs, namely how much conversion efficiency can be gained after the introduction of scattering layer. The increasing ratio of the conversion efficiency after adding a scattering layer in a wide range from 15% to 66.5% has been reported [15–20]. However, this parameter may not be suitable to evaluate the performance of the scattering layer, because the thickness of the TiO_2 NC layer may have significant influence on the scattering performance of the scattering layer. To our best knowledge, there are no systematic investigations on this issue.

In this study, RTCS process was used to prepare scattering layer for plastic-based DSCs to aim at improving both the efficiency and bending resistance of the plastic-based DSCs. The photovoltaic and mechanical properties of the DSCs were investigated. Moreover, the influence of the TiO_2 NC layer thickness on the performance of scattering layer was examined.

2. Experimental

2.1. Fabrication of photoanode

Commercially available nano-TiO_2 powder (P25, Degussa, 70% anatase and 30% rutile) of 25 nm in diameter and submicro-TiO_2 powder (anatase) of 100–200 nm in diameter were used in this study as shown in Fig. 1. The TiO_2 coatings were deposited by a home-developed RTCS system on indium-doped tin oxide coated polyethylene naphthalate (ITO-PEN, PECF-IP, 15 Ω sq^{-1}, Peccell) substrate. The RTCS system consists of a vacuum pump, a vacuum chamber, a powder feeder, an accelerating gas-feeding unit, a particle-accelerating nozzle, a two-dimension worktable and a control unit [21,22]. Helium gas was used as the accelerating gas at a pressure of 0.2 MPa. The chamber pressure during spraying was about 10^2–10^3 Pa. The standoff distance from the nozzle exit to the substrate surface was 10 mm. The relative traverse speed of the nozzle over the substrate was 20 mm s^{-1}. The photoanode

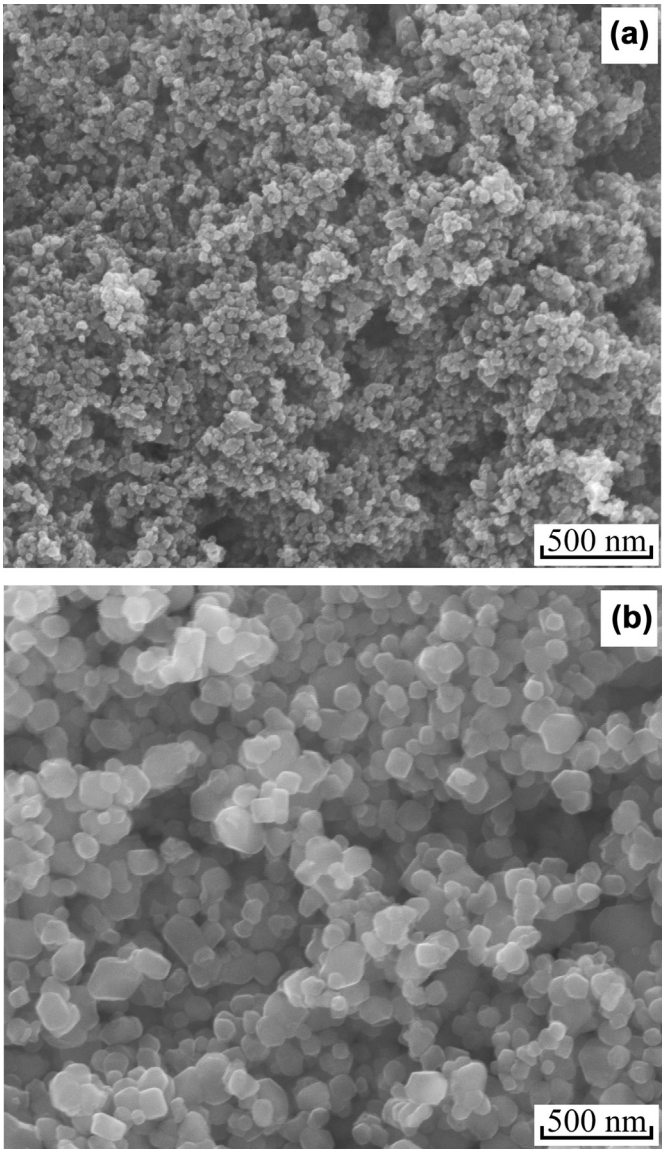

Fig. 1. Surface morphologies of the nano-TiO_2 powder (a) and submicro-TiO_2 powder (b).

consisted of TiO_2 NC layer with a thickness from 3 to 20 μm and a TiO_2 scattering layer of 10 μm. The TiO_2 NC layers were deposited at an accelerating gas flow rate of 7 L min^{-1}, while the TiO_2 scattering layer was deposited at an accelerating gas flow rate of 7.5 L min^{-1}. For comparison, a TiO_2 scattering layer was also prepared by a conventional spray deposition (SD) method using ethanol based submicro-TiO_2 particle suspension (5 wt.%) [23].

2.2. Fabrication of plastic-based DSCs

After deposition, the photoanode was annealed at 135 °C for 15 min. When cooled to 80 °C, the photoanode was immersed in an absolute ethanol solution of 0.3 mM N719 dye (Solaronix) for 24 h, followed by rinsing with absolute ethanol. After the photoanode was assembled with the plastic Pt CE using a 60 μm thick Surlyn film (1702, DuPont) as a spacer, the electrolyte solution was introduced into the cell through four holes pre-drilled on the back of the plastic CE, which were sealed up using a UV resin (Three-Bond). The electrolyte solution was composed of 0.6 M 1,2-dimethyl-3-propylimidazolium iodide (DMPII, Institute of Plasma

Physics, China), 0.05 M I_2 (Aldrich), 0.1 M LiI (Aldrich), and 0.5 M 4-*tert*-butylpyridine (Acros) in dehydrated acetonitrile (Aldrich).

2.3. Characterization

The microstructure of the TiO_2 scattering layer was studied by a field emission scanning electron microscope (FESEM, QUANTA 600F). The coating thickness was measured by a profilometer (XP-2, AMBIOS Technology, Inc., USA). The light-reflecting ability of the TiO_2 coating was evaluated by measuring the reflectance spectrum of the coating using a UV–Vis spectrophotometer equipped with an integrating sphere setup (JASCO V-570). The sphere, as well as the reference plates, is coated with $BaSO_4$. In this measurement, the TiO_2 scattering layer was deposited on a rigid conductive FTO-glass substrate (TEC 15, LOF), instead of the flexible ITO-PEN substrate, for convenient handling. Therefore, the measured reflectance spectrum was the combination of TiO_2 scattering layer and the FTO glass substrate.

The adhesion between the TiO_2 scattering layer and TiO_2 NC layer was evaluated by ultrasonic test using an ultrasonic cleaner (VGT-1730T, 120 W, Xi'an Coming Ultrasonic Equipment Instrument Co., Ltd. China). To facilitate the measurement, the TiO_2 scattering layers were deposited on FTO-glass substrate with a thickness of about 10 μm. The adhesion between the TiO_2 coating and the glass substrate was estimated by analyzing the coating detaching ratio, which was defined by the ratio of the detached area to the whole coating area, based on the surface morphology change of the coating after different ultrasonic test durations. The surface morphology was scanned by HP Scanjet 4890 scanner.

The photovoltaic performance of the plastic-based DSCs was measured using a solar simulator (100 mW cm^{-2}, Oriel 94023A, Newport) equipped with a Keithley 2400 digital source meter. The active area of photoanode was 0.4 cm^2. The monochromatic incident photon-to-current conversion efficiency (IPCE) of the plastic-based DSCs was measured by an IPCE measurement system (7-SCSpec, Beijing 7-star Optical Instruments Co. Ltd). To study the bending resistance of the plastic-based DSCs under outward bending mode, the DSCs were experienced a bending cycle as shown in Fig. 2. The bending test of the DSCs with and without scattering layer was carried out by a home-developed flexible solar cell bending tester, by which the bending conditions, including bending direction, bending radius and bending cycle, were accurately controlled [24].

3. Results and discussion

3.1. Light-reflecting ability of the TiO_2 scattering layer

Fig. 3 shows the surface morphologies of the TiO_2 scattering layers prepared by RTCS and SD method. As shown in Fig. 3a and b, the coating is formed by the stacking of TiO_2 particles with a size of 100–200 nm which is comparable to that of the spray powder (Fig. 1b). Moreover, it is obvious that the TiO_2 scattering layer prepared by SD method (Fig. 3c and d) shows the similar morphology to the RTCS-TiO_2 scattering layer.

The light-reflecting ability of the TiO_2 scattering layers is evaluated by measuring the reflectance of the TiO_2 scattering layers. Fig. 4 demonstrates the reflectance spectra of the TiO_2 NC layer and the TiO_2 scattering layers prepared by RTCS and SD method. As can be seen, all the TiO_2 scattering layers show much higher light-reflecting ability than the TiO_2 NC layer. Besides, the RTCS-TiO_2 scattering layer exhibits a relatively lower light-reflecting ability than the SD-TiO_2 scattering layer.

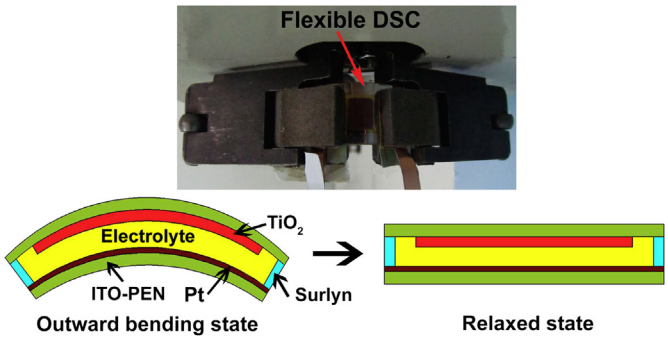

Fig. 2. The schematic of the plastic-based DSC under a bending cycle in an outward bending mode.

3.2. Adhesion between the substrate and the TiO_2 scattering layer

It should be noted that the adhesion between the TiO_2 scattering layer and the TiO_2 NC layer is essential for high performance plastic-based DSCs [25,26], since good connectivity between the TiO_2 scattering layer and TiO_2 NC layer is likely to enhance the electrical conductivity of the particle network and thereby efficient photon to electron conversion. However, it is difficult to test the adhesive strength between the TiO_2 NC layer and the TiO_2 scattering layer directly. In order to estimate the adhesive strength at the interface between the TiO_2 scattering layer and the TiO_2 NC layer, an ultrasonic test technique was used. The TiO_2 scattering layer was deposited on FTO-glass substrate, and the adhesive strength between the FTO-substrate and TiO_2 scattering layer was measured to indirectly estimate the adhesive strength between the TiO_2 NC layer and TiO_2 scattering layer.

Fig. 5 shows the surface morphologies of the scattering layers prepared by the SD and RTCS method after different ultrasonic test durations. As can be seen from Fig. 5a, the spalling off of a fraction of coating in flake (the dark contrast points or regions marked by black arrows) occurs to the SD-TiO_2 scattering layer, and becomes more serious with the increase of ultrasonic test duration. However, little spalling off occurs to the RTCS-TiO_2 scattering layer as shown in Fig. 5b. To facilitate the comparison, the relative adhesion index, which is defined as the ratio of the undetached area to the whole coating area, is used as shown in Fig. 6. After 120 s ultrasonic test, the RTCS-TiO_2 scattering layer shows a high relative adhesion index of about 97% between the coating and substrate. However, for the SD-TiO_2 scattering layer, the relative adhesion index is nearly 0% after ultrasonic test for 120 s, which indicates that nearly all the coating is peeled off from the substrate. These facts show that the adhesion between the particle–substrate interface in the SD-TiO_2 scattering layer is not sufficient.

During the RTCS process, some micro-sized powder particles directly impact on and adhere to the substrate, forming the first TiO_2 layer. The adhesion between the TiO_2 particles and the substrate surface is created by the pressure pulses owing to the high velocity spray particles impact on the substrate surface. Then the adhesion between the substrate and the first TiO_2 layer is strengthened by the tamping effect of the later approaching high velocity spray particles [27]. However, for the SD-TiO_2 scattering layer, the particles are mainly agglomerated together through physical bonding without high temperature sintering. In brief, the adhesion of the RTCS-TiO_2 scattering layer is better than the SD-TiO_2 scattering layer.

3.3. Dark current of the plastic-based DSCs

Several distinct photoanodes have been prepared to investigate the dark current of the plastic-based DSCs. The photoanode of DSCs consisted of a 10 μm thick TiO_2 NC layer and a 10 μm thick TiO_2

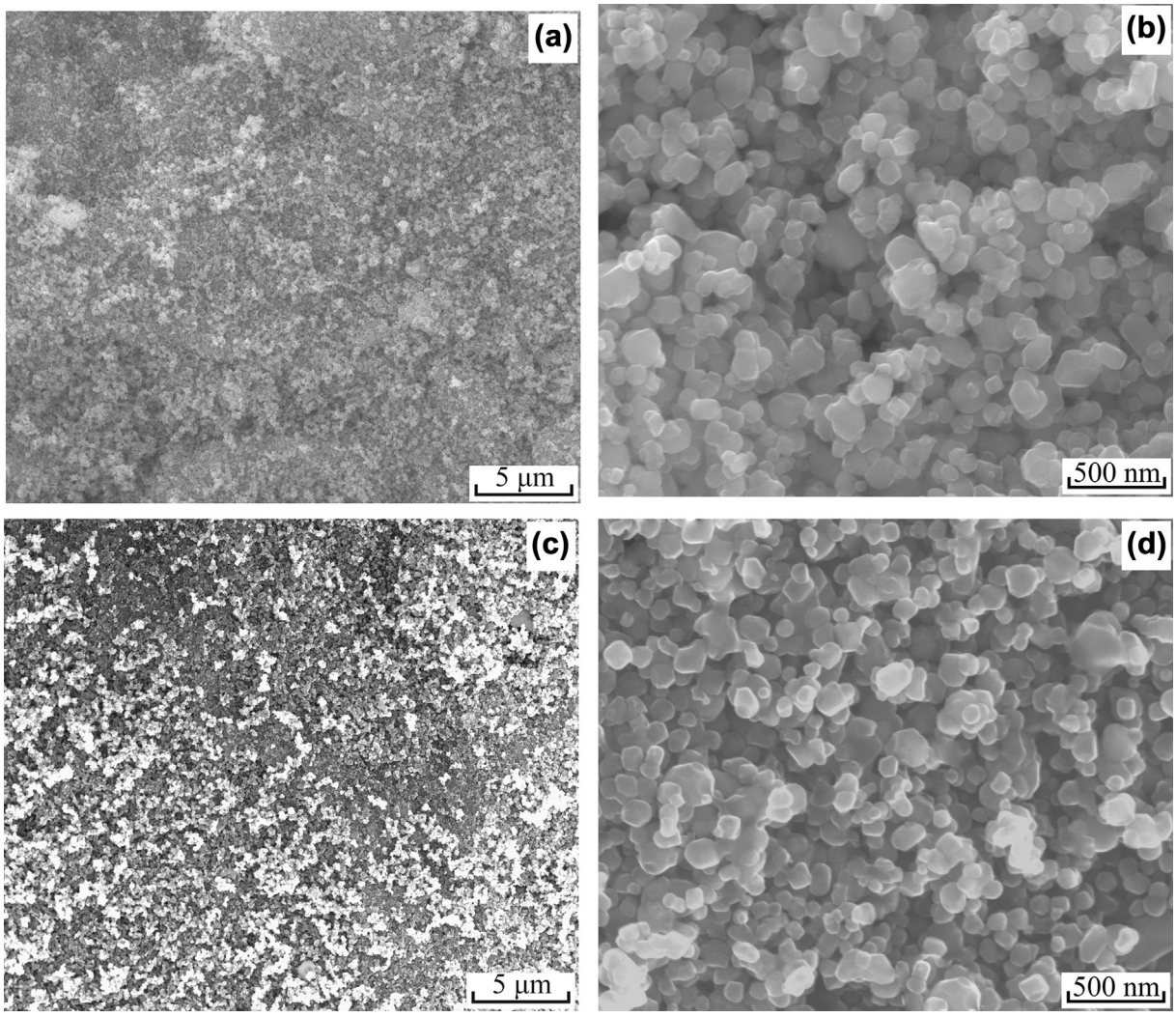

Fig. 3. Surface morphologies of TiO_2 scattering layers prepared by RTCS (a), (b) and SD method (c), (d).

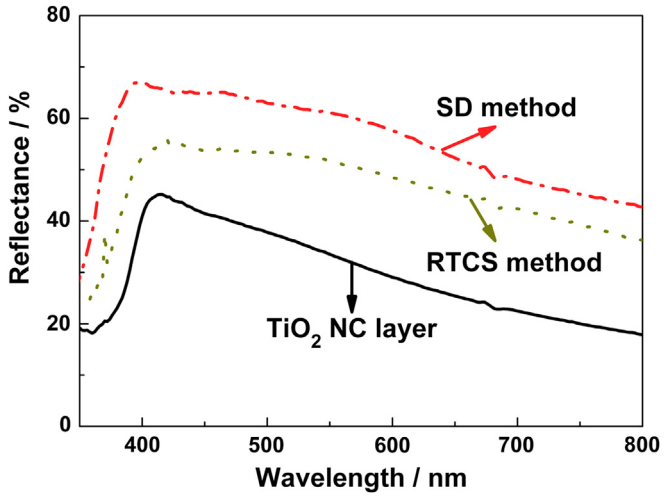

Fig. 4. Reflectance spectra of the TiO_2 NC layer and TiO_2 scattering layers prepared by RTCS and SD method.

scattering layer, which was deposited as an overlayer on the TiO_2 NC layer either by RTCS or SD method. Thus, three different photoanodes (NC, NC + RTCS, NC + SD) were constructed for the plastic-based DSCs. Fig. 7 shows the dark current of the plastic-based DSCs using three different photoanodes. The electron recombination rate at TiO_2/electrolyte interface can be estimated by the onset of dark current, which arises from the reduction of I_3^- ions by electrons in the conduction band of TiO_2 film [28]. At a certain voltage, such as 0.8 V, the dark current is nearly the same for the NC cell and NC + SD cell, while the dark current of the NC + RTCS cell is higher than other two cells. Since the dark current is determined by the effective surface area of the TiO_2 photoanode, this result means that the effective surface area of the photoanode is the same for the NC cell and NC + SD cell. Therefore, the adhesion between the SD-TiO_2 scattering layer and the TiO_2 NC layer should be weak, and the electrons cannot effectively transport from the TiO_2 NC layer to the SD-TiO_2 scattering layer. On the other hand, the higher dark current of the NC + RTCS cell implies that the electrons can effectively transport from the TiO_2 NC layer to the RTCS-TiO_2 scattering layer, and thereby recombine with the I_3^- ions in the electrolyte. The effective recombination surface area of the NC + RTCS cell is increased, and consequently the dark current is increased. This result well reflects that the adhesion between the

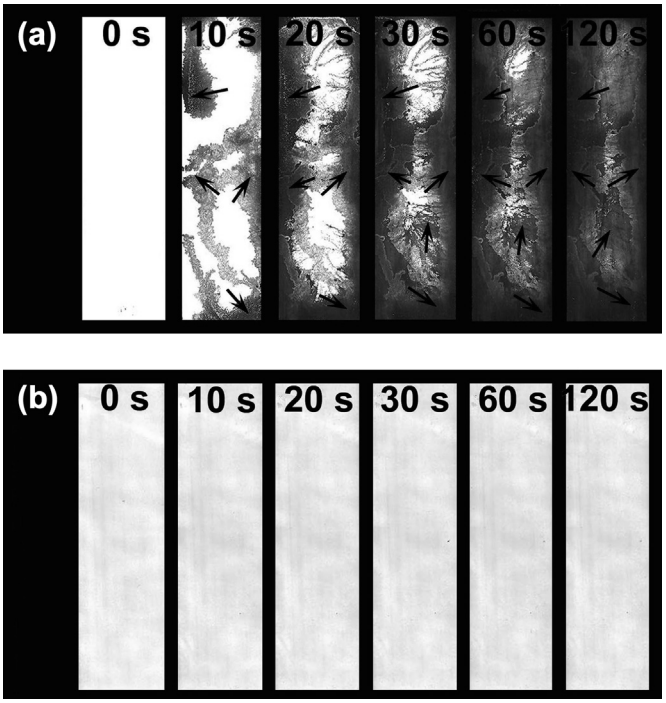

Fig. 5. Surface morphologies of the TiO_2 scattering layers prepared by SD (a) and RTCS method (b) after different ultrasonic test durations.

RTCS-TiO_2 scattering layer and TiO_2 NC layer is better than the adhesion between SD-TiO_2 NC layer and TiO_2 NC layer.

3.4. Photovoltaic performance of the plastic-based DSCs

Fig. 8a shows the photocurrent–voltage curves of the plastic-based DSCs using three different photoanodes and the corresponding photovoltaic parameters are listed in Table 1. The energy conversion efficiency (η) is mainly determined by the short-circuit current density (J_{SC}). It is obvious that after adding a TiO_2 scattering layer to the surface of TiO_2 NC layer, the efficiency is significantly improved. This result is attributed to the improved light confinement within the bi-layer photoanode. Moreover, compared to the

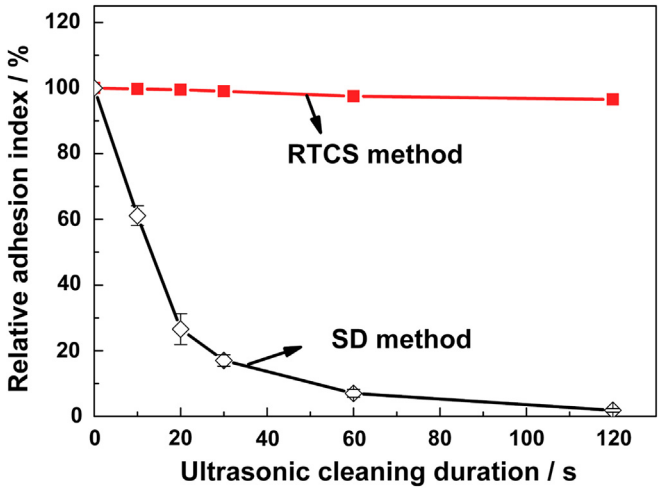

Fig. 6. Relative adhesion index of the TiO_2 scattering layers prepared by RTCS and SD method as a function of ultrasonic test duration.

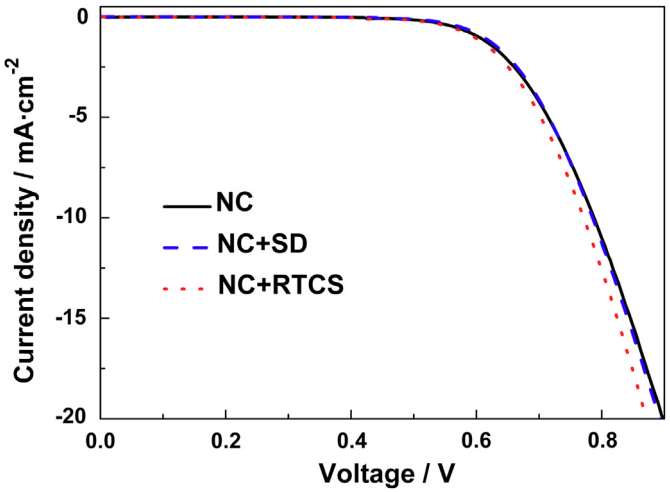

Fig. 7. Dark current of the plastic-based DSCs using different photoanodes.

NC + SD cell, the NC + RTCS cell exhibits much higher conversion efficiency. Taking the relatively lower light-reflecting ability of the RTCS-TiO_2 scattering layer into account, the higher efficiency of the NC + RTCS cell can be attributed to the good adhesion between the

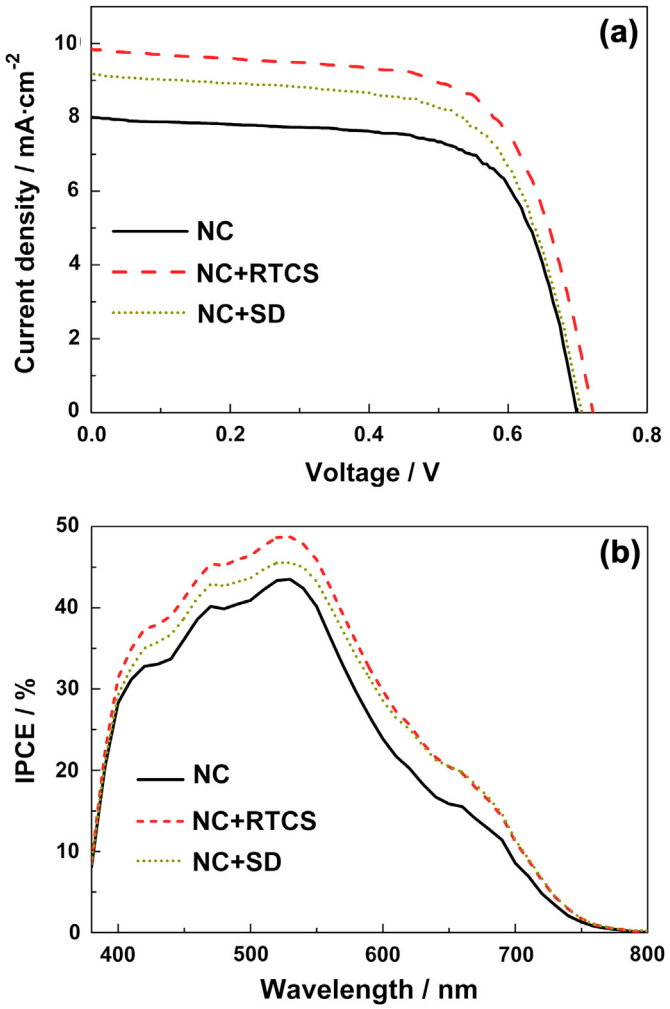

Fig. 8. *I–V* curves (a) and IPCE spectra (b) of the plastic-based DSCs using different photoanodes.

Table 1
Photovoltaic performance of the plastic-based DSCs using different photoanodes.

Photoanode	JSC (mA cm^{-2})	VOC (mV)	FF	η (%)
NC	7.98 ± 0.24	705 ± 7	0.69 ± 0.01	3.88 ± 0.13
NC + RTCS	9.74 ± 0.20	725 ± 6	0.67 ± 0.01	4.70 ± 0.13
NC + SD	9.16 ± 0.21	710 ± 5	0.66 ± 0.01	4.29 ± 0.18

RTCS-TiO_2 scattering layer and TiO_2 NC layer. In addition, it is known that the TiO_2 scattering layer can also uptake dye molecules. These results mean that the photo-induced electrons in the RTCS-TiO_2 scattering layer can effectively transport to the TiO_2 NC layer and thereby improve the overall conversion efficiency. As for the NC + SD cell, the photo-induced electrons in the SD-TiO_2 scattering layer cannot effectively transport to the TiO_2 NC layer owing to the poor adhesion between the TiO_2 NC layer and SD-TiO_2 scattering layer. Therefore, the adhesion between the TiO_2 NC layer and TiO_2 scattering layer is mainly responsible for the difference in the conversion efficiency of different DSCs. Besides, the IPCE spectra, which offer detailed information on the light harvest of the solar cells, were also measured as shown in Fig. 8b. It is clear that the overall IPCE increases considerably by the introduction of scattering layers, resulting in higher J_{SC} values. Obviously, the device using RTCS-TiO_2 scattering layer possesses higher IPCE than the device using SD-TiO_2 scattering layer in the wavelength range from 400 to 700 nm, resulting from the improved adhesion properties between the TiO_2 scattering layer and TiO_2 NC layer.

3.5. *Photovoltaic performance of the plastic-based DSCs under alternating outward bending*

The flexibility is one of the most important features for the application of plastic-based DSCs [12,24,29]. In this study, the bending resistance of the plastic-based DSCs using RTCS-TiO_2 scattering layer and SD-TiO_2 scattering layer was examined with a home-developed flexible solar cell bending tester. It should be noted that, the electrolyte is still in the solar cells and no leakage occurs after the bending test. Fig. 9 exhibits the normalized efficiency of the plastic-based DSCs with and without RTCS-TiO_2 scattering layer and SD-TiO_2 scattering layer as a function of bending cycle. The normalized efficiency is defined as the ratio of the efficiency of the solar cells with a scattering layer to that of the NC cell before bending test. As can be seen in Fig. 9, the normalized efficiency is nearly unchanged with the increase of bending cycle for the NC cell, showing a good particle connection of the TiO_2 NC layer. However, for the NC + SD cell, the normalized efficiency decreases with the increase of bending cycle. Moreover, after 10,000 bending cycles, the efficiency of the NC + SD cell is nearly the same as that of the NC cell, implying that the scattering layer fails to improve the efficiency of the plastic-based DSCs. To explore the reason for the failure of SD-TiO_2 scattering layer, the surface morphologies of the photoanode of NC + SD cell before and after 10,000 bending cycles were studied as shown in Fig. 10. As can be seen in Fig. 10, the SD-TiO_2 scattering layer is peeled off from the TiO_2 NC layer after 10,000 bending cycles, which is the main reason for the failure of SD-TiO_2 scattering layer. In addition, for the NC + RTCS cell, the normalized efficiency is also unchanged with the increase of bending cycle, implying the good connection between the particles in RTCS-TiO_2 scattering layer and good adhesion between the RTCS-TiO_2 layer and TiO_2 NC layer. Therefore, it can be concluded that the adhesion between the scattering layer

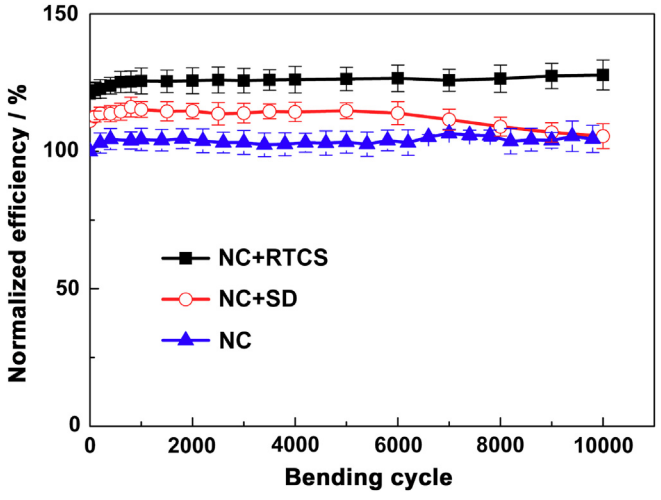

Fig. 9. Normalized efficiency of the plastic-based DSCs using different photoanodes under outward bending mode as a function of bending cycle.

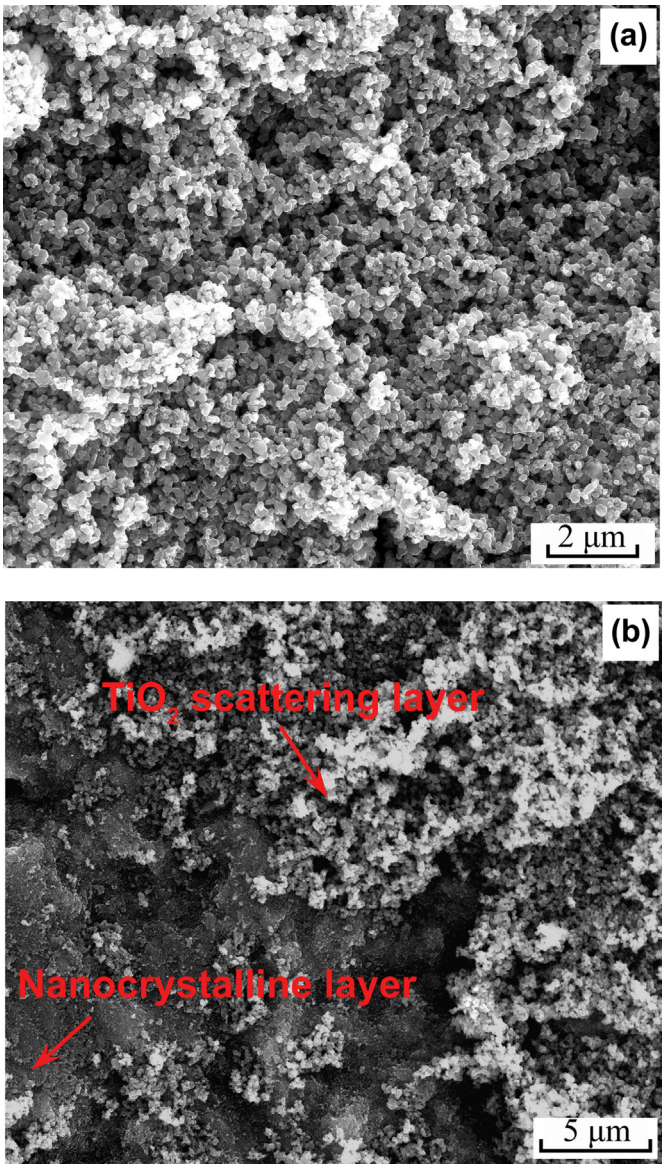

Fig. 10. Surface morphologies of the photoanode of NC + SD cell before (a) and after (b) 10,000 cycles outward bending.

and the TiO_2 NC layer is essential for the improved efficiency of plastic-based DSCs under bending condition, and the NC + RTCS cell exhibits higher bending resistance to failure than the NC + SD cell.

3.6. Effect of TiO_2 NC layer thickness on the efficiency of scattering layer

Another issue should be noted is that in many reports the increasing ratio of conversion efficiency was used to evaluate the effect of scattering layer [16]. From the literature [15–20], the reported increasing ratio in a wide range from 15% to 66.5% can be found. However, the question is whether the increasing ratio reported in different literature is comparable for different DSCs with a scattering layer or not.

When the sunlight is illuminated on the plastic-based DSCs from the photoanode side, a loss of about 20% of the light will occur based on the absorption and reflection of the ITO-PEN substrate. The transmitted light will then be absorbed by the dye molecules on the TiO_2 NC layer. The more the amount of dye molecules, the more sunlight is absorbed. The unabsorbed light will be scattered back to the TiO_2 NC layer by the scattering layer, which in turn improves the absorption efficiency and thereby the conversion efficiency of the solar cells. It is known that the amount of the dye molecules increased nearly linearly with the thickness of the TiO_2 NC layer. In principle, the light-scattering efficiency of scattering layer will be proportional to the portion of the transmitted light through the TiO_2 NC layer and also to its reflectance value [18]. Therefore, the intensity of scattered light will be stronger for a thinner TiO_2 NC layer than for a thicker TiO_2 NC layer.

Based on the discussion above, the effect of the TiO_2 NC layer thickness on the scattering efficiency of scattering layer was systematically studied. Fig. 11 shows the J_{SC} and efficiency of the plastic-based DSCs with and without RTCS-TiO_2 scattering layer as a function of the TiO_2 NC layer thickness. From Fig. 11, it is obvious that the J_{SC} and efficiency of both the plastic-based DSCs with and without scattering layer exhibits a similar dependency on the TiO_2 NC layer thickness. The J_{SC} increases with the increase of the TiO_2 NC layer thickness and consequently the conversion efficiency until both reaching the maximum value at a thickness of 15 μm. When the thickness of the TiO_2 NC layer is larger than 15 μm, the J_{SC} and the conversion efficiency tend to decrease with further increase in the TiO_2 NC layer thickness, which may be due to the limited I_3^- ions diffusion in the porous photoanode. Moreover, the estimated increasing ratio for the J_{SC} and conversion efficiency of the plastic-based DSCs with a RTCS-TiO_2 scattering layer was calculated as shown in Fig. 12. As can be seen in Fig. 12, the increase of conversion efficiency was mainly contributed by the increase of J_{SC}. Moreover, the efficiency increasing ratio decreases from 60% to 15% with the increase of the TiO_2 NC layer thickness from 6 to 15 μm. This result indicates that the thickness of the TiO_2 NC layer significantly influences the effect of the scattering layer. The wide range of efficiency increasing ratio is consistent with these literature as discussion above. Finally, it can be concluded that the increasing ratio of conversion efficiency by scattering layer is incomparable among the solar cells using TiO_2 NC layer with different thicknesses.

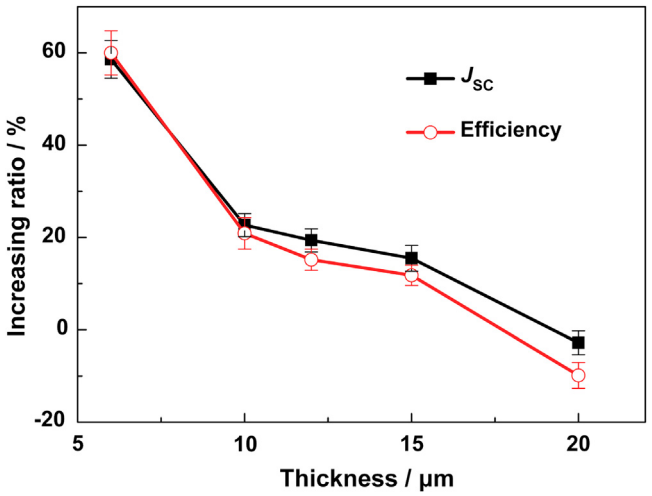

Fig. 12. The increasing ratio of the J_{SC} and efficiency of the plastic-based DSCs with RTCS-TiO_2 scattering layer and as a function of the TiO_2 NC layer thickness.

By using a TiO_2 NC layer with an optimized thickness (15 μm), the J_{SC}, V_{OC}, FF of the plastic-based DSCs are 11.4 mA cm^{-2}, 0.71 V, 0.65, respectively, and a highest efficiency of 5.24% is achieved. Fig. 13 shows the IPCE spectra of the plastic-based DSCs using 15 μm TiO_2 NC layer with and without RTCS-TiO_2 scattering layer. The two

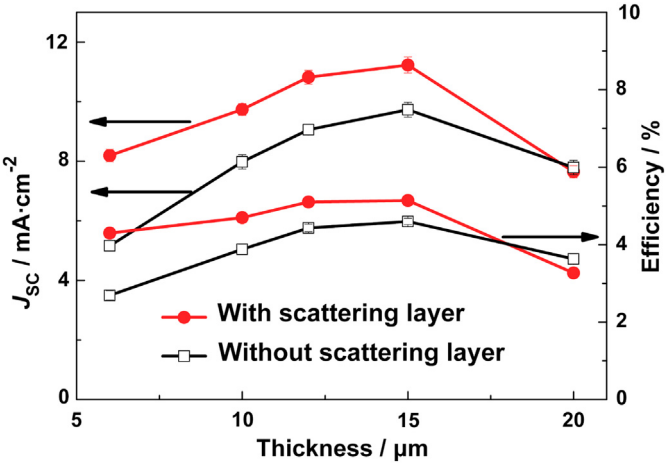

Fig. 11. J_{SC} and efficiency of the plastic-based DSCs with and without RTCS-TiO_2 scattering layer as a function of the TiO_2 NC layer thickness.

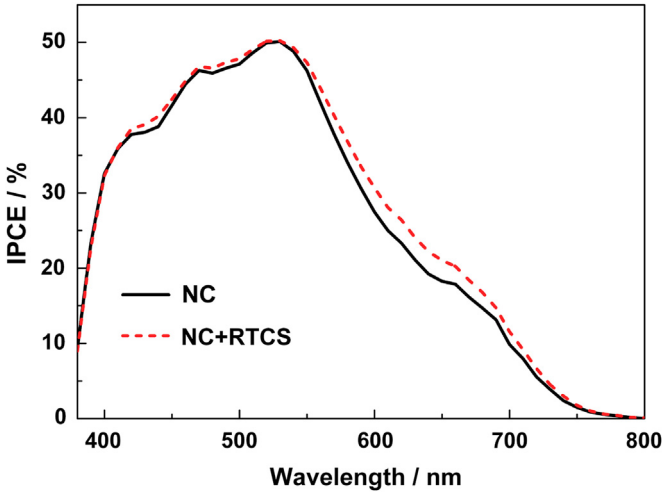

Fig. 13. IPCE spectra of the plastic-based DSCs with and without RTCS-TiO_2 scattering layer. The thickness of the TiO_2 NC layer is 15 μm.

devices present nearly the same IPCE in the short wavelength range from 400 to 550 nm. However, the IPCE for the plastic-based DSC with a scattering layer is slightly higher in the long wavelength range from 550 to 750 nm. This can be explained by the following reasons. For the DSC using TiO_2 NC layer with an optimized thickness, the light in the short wavelength (400–550 nm) is almost absorbed according to the characteristic of the N719 dye used in this study [30]. The transmitted light from the TiO_2 NC layer is composed mostly of the unabsorbed light in the long wavelength (550–750 nm), which will then be scattered back to the TiO_2 NC layer by the RTCS-TiO_2 scattering layer. Therefore, the IPCE for the solar cell using TiO_2 NC layer with optimized thickness with RTCS-TiO_2 scattering layer is higher in the long wavelength range from 550 to 750 nm and nearly the same in the short wavelength range from 400 to 550 nm compared to the IPCE of the solar cell without RTCS-TiO_2 scattering layer.

4. Conclusions

Room temperature cold spraying (RTCS) and spray deposition (SD) method were used to prepare light scattering layers for plastic-based DSCs with submicro-TiO_2 powder. Both the RTCS-TiO_2 scattering layer and the SD-TiO_2 scattering layer showed a much higher light-reflecting ability than the TiO_2 NC layer. The adhesion between the TiO_2 scattering layer and TiO_2 NC layer for the NC + RTCS cell was higher than the NC + SD cell, and subsequently contributed to a higher efficiency and better bending resistance than the NC + SD cell. Moreover, it was found that the increasing ratio of conversion efficiency of the plastic-based DSCs with a scattering layer significantly decreased with increasing the thickness of TiO_2 NC layer. By using the TiO_2 NC layer with an optimized thickness of 15 μm, a highest efficiency of 5.24% was achieved for the plastic-based DSC with a RTCS-TiO_2 scattering layer.

Acknowledgments

The work was supported by the National Science Foundation of China (No.: 51072160), Program for New Century Excellent Talents in University (No. NCET-08-0443), Program for Young Excellent Talents in Shaanxi Province (No. 20kjxx32), and the Fundamental Research Funds for the Central Universities.

References

[1] T. Yamaguchi, N. Tobe, D. Matsumoto, T. Nagai, H. Arakawa, Sol. Energy Mater. Sol. Cells 94 (2010) 812–816.
[2] X.L. He, M. Liu, G.J. Yang, S.Q. Fan, C.-J. Li, Appl. Surf. Sci. 258 (2011) 1377–1384.
[3] L. Yang, Y. Lin, J.G. Jia, X.R. Xiao, X.P. Li, X.W. Zhou, J. Power Sources 182 (2008) 370–376.
[4] J.G. Yu, J.J. Fan, L. Zhao, Electrochim. Acta 55 (2010) 597–602.
[5] J.G. Yu, J.J. Fan, K.L. Lv, Nanoscale 2 (2010) 2144–2149.
[6] W.H. Chiu, K.M. Lee, W.F. Hsieh, J. Power Sources 196 (2011) 3683–3687.
[7] W.K. Tu, C.J. Lin, A. Chatterjee, G.H. Shiau, S.H. Chien, J. Power Sources 203 (2012) 297–301.
[8] J.G. Yu, J.J. Fan, B. Cheng, J. Power Sources 196 (2011) 7891–7898.
[9] P. Chen, Y.W. Lo, T.L. Chou, J.M. Ting, J. Electrochem. Soc. 158 (2011) H1252–H1257.
[10] J.G. Yu, Q.L. Li, Z. Shu, Electrochim. Acta 56 (2011) 6293–6298.
[11] Y.W. Jang, Y.K. Kim, H.W. Park, D.H. Won, S.E. Cho, W.P. Hwang, K.S. Jung, M.R. Kim, J.K. Lee, Mol. Cryst. Liq. Cryst. 538 (2011) 240–248.
[12] C.Y. Jiang, X.W. Sun, K.W. Tan, G.Q. Lo, A.K.K. Kyaw, D.L. Kwong, Appl. Phys. Lett. 92 (2008) 143101.
[13] S.Q. Fan, C.-J. Li, G.J. Yang, J.C. Gao, L.Z. Zhang, C.X. Li, Y.Y. Wang, Key Eng. Mater. 373–374 (2008) 742–745.
[14] G.J. Yang, C.-J. Li, K.X. Liao, X.L. He, S. Li, S.Q. Fan, Thin Solid Films 519 (2011) 4709–4713.
[15] C.S. Chou, M.G. Guo, K.H. Liu, Y.S. Chen, Appl. Energy 92 (2012) 224–233.
[16] K. Fan, W. Zhang, T.Y. Peng, J.N. Chen, F. Yang, J. Phys. Chem. C 115 (2011) 17213–17219.
[17] X.C. Zhao, H. Lin, X. Li, J.B. Li, Mater. Lett. 65 (2011) 1157–1160.
[18] I.G. Yu, Y.J. Kim, H.J. Kim, C. Lee, W.I. Lee, J. Mater. Chem. 21 (2011) 532–538.
[19] Y.C. Park, Y.J. Chang, B.G. Kum, E.H. Kong, J.Y. Son, Y.S. Kwon, T. Park, H.M. Jang, J. Mater. Chem. 21 (2011) 9582–9586.
[20] J. Jiang, J. Zhang, F. Gu, W. Shao, C.Z. Li, M.K. Lu, Particuology 9 (2011) 222–227.
[21] S.Q. Fan, C.-J. Li, C.X. Li, G.J. Liu, G.J. Yang, L.Z. Zhang, Mater. Trans. 47 (2006) 1703–1709.
[22] S.Q. Fan, C.-J. Li, G.J. Yang, L.Z. Zhang, J.C. Gao, Y.X. Xi, J. Therm. Spray Technol. 16 (2007) 893–897.
[23] J. Halme, M. Toivola, A. Tolvanen, P. Lund, Sol. Energy Mater. Sol. Cells 90 (2006) 872–886.
[24] X.L. He, M. Liu, G.J. Yang, H.L. Yao, S.Q. Fan, C.-J. Li, J. Power Sources 226 (2013) 173–178.
[25] H.C. Weerasinghe, P.M. Sirimanne, G.V. Franks, G.P. Simon, Y.B. Cheng, J. Photochem. Photobiol. A Chem. 213 (2010) 30–36.
[26] K. Shin, Y. Jun, J.H. Moon, J.H. Park, ACS Appl. Mater. Inter. 2 (2010) 288–291.
[27] P.H. Gao, Y.G. Li, C.-J. Li, G.J. Yang, C.X. Li, J. Therm. Spray Technol. 17 (2008) 742–749.
[28] S. Ito, P. Liska, P. Comte, R. Charvet, P. Pechy, U. Bach, L. Schmidt-Mende, S.M. Zakeeruddin, A. Kay, M.K. Nazeeruddin, M. Gratzel, Chem. Commun. (2005) 4351–4353.
[29] Y. Li, K. Yoo, D.K. Lee, J.H. Kim, N.G. Park, K. Kim, M.J. Ko, Curr. Appl. Phys. 10 (2010) E171–E175.
[30] N.N. Bwana, Nano Res. 1 (2008) 483–489.